



Published in final edited form as:

*J Am Soc Mass Spectrom.* 2018 July ; 29(7): 1505–1511. doi:10.1007/s13361-018-1946-6.

## An Internal Standard for Assessing Phosphopeptide Recovery from Metal Ion/Oxide Enrichment Strategies

Joao A. Paulo<sup>1,#</sup>, Jose Navarrete-Perea<sup>1</sup>, Alison R. Erickson<sup>1</sup>, Jeffrey Knott<sup>2</sup>, and Steven P. Gygi<sup>1,#</sup>

<sup>1</sup>Department of Cell Biology, Harvard Medical School, Boston, MA 02115, United States

<sup>2</sup>Cell Signaling Technology, Danvers, MA 01923, USA

### Abstract

Phosphorylation-mediated signaling pathways have major implications in cellular regulation and disease. However, proteins with roles in signaling pathways are frequently less abundant and phosphorylation is often sub-stoichiometric. As such, the efficient enrichment and subsequent recovery of phosphorylated peptides is vital. Mass spectrometry-based proteomics is a well-established approach for quantifying thousands of phosphorylation events in a single experiment. We designed a peptide internal standard-based assay directed toward sample preparation strategies for mass spectrometry analysis to understand better phosphopeptide recovery from enrichment strategies. We coupled mass-differential tandem mass tag (mTMT) reagents (specifically, TMTzero and TMTsuper-heavy), nine mass spectrometry-amenable phosphopeptides (phos9), and peak area measurements from extracted ion chromatograms to determine phosphopeptide recovery. We showcase this mTMT/phos9 recovery assay by evaluating three phosphopeptide enrichment workflows. Our assay provides data on the recovery of phosphopeptides, which complement other metrics, namely the number of identified phosphopeptides and enrichment specificity. Our mTMT/phos9 assay is applicable to any enrichment protocol in a typical experimental workflow irrespective of sample origin or labeling strategy.

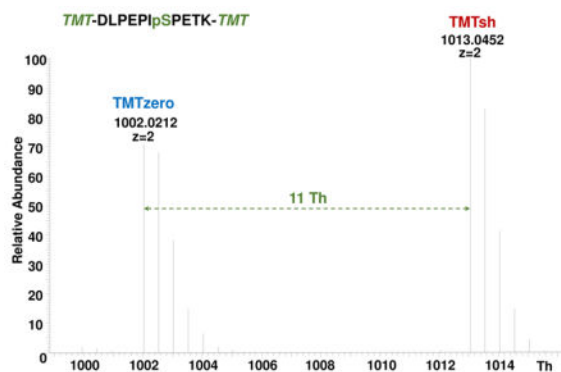
### Graphical Abstract

---

<sup>#</sup>Corresponding authors: Joao A. Paulo, Department of Cell Biology, 240 Longwood Ave., Harvard Medical School, Boston, Massachusetts 02115, USA, joao\_paulo@hms.harvard.edu. Steven P. Gygi, Department of Cell Biology, 240 Longwood Ave., Harvard Medical School, Boston, Massachusetts 02115, USA, sgygi@hms.harvard.edu.

#### Competing interest

The authors acknowledge no competing interests.



## Keywords

TMT super-heavy; TMTsh; TMT0; TMTzero; Lumos; phosphorylation; mTRAQ

## INTRODUCTION

Mass spectrometry-based proteomics techniques are often adapted to measure changes in global phosphorylation events [1–6]. Phosphorylation cascades contribute to a plethora of cellular functions through intricate networks of proteins in signaling pathways [7–10]. As shifts in phosphorylation events are more numerous than protein alterations, targeting single proteins does not sufficiently address global cellular mechanisms [1, 11, 12]. As such, the comprehensive study of the phosphoproteome relies heavily on proper phosphopeptide enrichment. However, no single universal phosphoproteomic enrichment methodology exists currently. Several enrichment strategies have been applied successfully in mass spectrometry-based investigations, including selective interaction with metals in the form of chelated metal ions [13–18] or metal oxides [18]. Bead composition and peptide-to-bead ratios have been contributing factors to the performance of these methods. As phosphopeptides are generally sub-stoichiometric, efficient enrichment and recovery are critical to achieving deep phosphoproteome coverage.

Typically, Tandem Mass Tags (TMT) reagents are used for multiplexed, isobaric labeling, as in TMT-MS3 workflows [1, 11, 12]. However, four variants of TMT exist, each with distinct masses: TMTzero (224.152 Da), TMT2-plex (225.155 Da), TMT6/10/11-plex (229.163 Da), and TMTsuperheavy (235.177 Da). These amine tag variants, which we term mTMT (mass-differential tandem mass tag) are not isobaric, but nevertheless co-elute and can be used for MS1-based quantification, similar to mTRAQ [19]. To reduce the potential of overlapping isotopic envelopes, we use the two most distant mTMT variants, TMTzero with no stable isotopes and TMTsuper-heavy (TMTsh) with 11 stable isotopes. Peptides labeled with TMTzero or TMTsh do not interfere with standard TMT2/6/10/11-plex quantification strategies and can be used to optimize both label-free and isobaric labeled phosphopeptide enrichment protocols.

Here we developed an assay to measure phosphopeptide recovery by combining mTMT (i.e., TMTzero and TMTsh) and a cocktail of mass spectrometry-amenable phosphopeptide

internal standards, hereafter referred to as phos9. As proof-of-principle, we compared three enrichment methods using the mTMT/phos9 recovery assay: two Fe-NTA (nitrilotriacetic acid)-based IMAC (immobilized metal affinity chromatography) protocols and one TiO<sub>2</sub>-based MOAC (metal oxide affinity chromatography) protocol. We report the number of phosphopeptides and enrichment specificity for each method. In addition, the assay allowed us to determine the percent recovery of phosphorylated peptides. This versatile mTMT/phos9 recovery assay is useful in optimizing virtually any phosphoproteome enrichment strategy.

## METHODS

We developed a method to evaluate phosphopeptide recovery by analyzing chromatographic peak area measurement differences of non-isobaric, mass-differential TMT (mTMT)-labeled phosphopeptide internal standards (phos9) that are added before and after enrichment. We assembled two equi-molar cocktails of phos9 peptides, one labeled with TMTzero and another with TMTsh. We applied our recovery assay to three commercial phosphopeptide enrichment workflows: High-Select Fe-NTA Phosphopeptide Enrichment Kit (IMAC1; High-Select), Fe-NTA Phosphopeptide Enrichment Kit (IMAC2; Fe-NTA), and High-Select TiO<sub>2</sub> Phosphopeptide Enrichment Kit (TiO<sub>2</sub>). For the assay, we added approximately 0.5 pmol of each TMTzero-labeled phos9 peptides to 1mg of tryptic peptides from human whole cell lysate, and we performed the enrichment according to manufacturer's instructions. Following enrichment, 0.5 pmol of each TMTsh-labeled phos9 peptide were added to the eluent. The sample was then desalted and subjected to LC-MS/MS. Our mass spectrometry data were collected in data-dependent acquisition (DDA) mode using a Q-Exactive mass spectrometer (Thermo Fisher Scientific) coupled to a Famos Autosampler (LC Packings) and an Accela600 liquid chromatography (LC) pump (Thermo Fisher Scientific). Approximately 1 µg of peptide were loaded onto an Accucore C18 column (Thermo Fisher Scientific) and separated over a 90-min gradient. Mass spectra were processed with a SEQUEST-based software pipeline [5] and SkyLine 3.7 [20, 21]. SEQUEST searches were performed with phosphorylation at serine, threonine, and tyrosine residues (+79.966 Da) set as a variable modification. PSMs were identified, quantified, and collapsed to a 1% peptide false discovery rate (FDR) and collapsed further to a final protein-level FDR of 1% [22, 23]. Peak areas from the mTMT-labeled phos9 peptides were extracted and quantified with Skyline. Expanded experimental methods are available in the Supplementary Methods. The mass spectrometry proteomics data have been deposited to the ProteomeXchange Consortium via the PRIDE partner repository with the dataset identifier PXD008966.

## RESULTS AND DISCUSSION

We and others have noted enrichment strategy-specific differences in phosphopeptide recovery. As such, we designed a mass spectrometry-based internal standard assay to assess phosphopeptide recovery across enrichment methods. We first synthesized a set of nine mass spectrometry-amenable phosphopeptides, collectively termed phos9 (Fig. 1A). We chose phosphopeptides from a previously published *S. cerevisiae* dataset [11]. Selection criteria included a length of 10–18 amino acids, no more than one missed cleavage, no methionine (to avoid oxidation artifacts) or cysteine (to avoid alkylation artifacts) residues. These

peptides were also consistently detected across mass spectrometry-based phosphorylation experiments. We then labeled these peptides with non-isobaric mass-differential tandem mass tag (mTMT) reagents (TMTzero and TMTsh) (Fig. 1B). For doubly-charged arginine-terminating peptides with no internal lysines, the mass difference between these mTMT tags is ~5.5 Th, while this difference is ~11.0 Th for lysine-terminating peptides (due to the TMT label on the C-terminal lysine in addition to the N-terminus) (Fig. 1C). The chromatograms illustrating peptide retention time showed that the differentially-labeled peptides co-elute (Supplemental Fig. 1). From here, peak area differences were calculated for differentially-tagged phosphopeptides. The analytical workflow of the mTMT/phos9 recovery assay is outlined in Fig. 2A.

As proof-of-principle, we subjected 1 mg aliquots of human whole cell lysate to three phosphopeptide enrichment strategies in triplicate. To each sample, we added a cocktail of TMTzero-labeled phos9 prior to enrichment, and a second cocktail of TMTsh-labeled phos9 peptides following enrichment. We used SkyLine 3.7 to extract ion chromatograms (Fig. 2B) and to calculate peak areas (Fig. 2C) for each phosphopeptide. Important parameters to assess for any phosphopeptide experiment included the total number of phosphopeptides, the enrichment specificity, and the phosphopeptide recovery.

While the total number of phosphopeptides and the enrichment specificity (defined as the ratio of phosphorylated peptides to total peptides identified) can be determined without modification to enrichment strategies, a more directed assay was necessary to assess phosphopeptide recovery. The classical strategy of using radioactive isotope-labeled peptides has major deterrents associated with potential health risks and stringent regulations. To establish a more universally applicable method, we designed a recovery assay based on mTMT stable isotope-labeled phos9. By flanking the enrichments with these two cocktails, we can use area under the chromatographic peak ratios of the “heavy” (TMTsh) to “light” (TMTzero) peptides to estimate the recovery efficiency of each method. We calculated the percent recovery for the phosphorylated phos9 peptides for each method tested (Fig. 3A). The recovery of the phos9 peptides was on average  $78.3 \pm 7\%$  for IMAC1 (High-Select),  $56.8 \pm 18\%$  for IMAC2 (Fe-NTA) and  $22.9 \pm 16\%$  for  $\text{TiO}_2$ . When comparing the three methods, the High-Select workflow yielded the most promising results in our hands, providing the highest number of phosphorylated peptides recovered. The spectra collected were also subjected to database searching using the Sequest algorithm from which traditional phosphopeptide metrics, i.e., the number of phosphopeptides and percent enrichment, can be assessed from the actual sample.

The Sequest search revealed that IMAC resin-based strategies identified the highest number of phosphorylated peptides among the strategies tested. The High-Select and Fe-NTA workflows identified on average  $5,616 \pm 204$  and  $4,931 \pm 292$  phosphopeptides, respectively, while  $\text{TiO}_2$  identified only  $2,684 \pm 305$  phosphopeptides (Fig. 3B, **bars**). However, this trend was different with regard to enrichment specificity. The average enrichment specificity was higher in the  $\text{TiO}_2$  and High-Select methods, with  $95.5 \pm 2\%$  and  $90.2\% \pm 6\%$ , respectively, whereas this value was only  $45.5\% \pm 2\%$  for the Fe-NTA enrichment workflow (Fig. 3B, **dots**). We note that the IMAC resins differed substantially in enrichment specificity. This scenario was predictable as decreased enrichment specificity (as in the Fe-NTA workflow)

will decrease the number of quantified, phosphorylated peptides, as more non-phosphorylated peptides are available for sequencing. Compared to High-Select, the Fe-NTA resin identified nearly 10% fewer phosphopeptides, which is likely impacted by 50% less enrichment specificity (Fig. 3B, **dots**). Although the modality of enrichment (IMAC) was equivalent between High-Select and Fe-NTA, the proprietary buffers used in each workflow were distinct. Conventional IMAC material exhibits relatively low enrichment specificity as non-phosphorylated peptides with multiply acidic residues tend to show strong nonspecific binding [24]. However, protonating carboxylate moieties at low pH decreases such binding. An altered buffer composition may explain the improvement in performance of the High-Select workflow over its Fe-NTA predecessor. When comparing the TiO<sub>2</sub> and High-Select workflows, we observed that although both methods have high enrichment specificity, High-Select identified over twice as many phosphopeptides. We proposed that this discrepancy was a result of recovery, that is, fewer phosphopeptides are eluted from the TiO<sub>2</sub> beads compared to the High-Select IMAC beads. The data for the number of phosphopeptides, the enrichment specificity, and the phosphopeptide recovery were summarized in Fig. 3C. Our assay could be used to track the phos9 peptides through multiple elutions. As the assay can be applied to any enrichment strategy, one can gain further insight into the binding kinetics of the phosphopeptides to the matrix. Upon discovering where phosphopeptides are lost, buffers and/or binding conditions can be altered so as to improve the enrichment strategy.

Our mTMT/phos9 assay can be applied seamlessly to any enrichment protocol regardless of sample origin or labeling strategy employed. Coincidentally, previous studies have shown the complementarity of MOAC and IMAC methods in efforts to obtain a comprehensive phosphoproteome [25]. As such, using two or more methods in tandem or coupled to another enrichment strategy [26], including those using motif-specific antibodies [27], may deepen our coverage of the phosphoproteome. In SMOAC (Sequential enrichment of Metal Oxide Affinity Chromatography), peptides not binding to TiO<sub>2</sub> are enriched further with Fe-NTA [28]. In addition, ion exchange chromatography, for example, SCX (strong cation exchange) [29] has been used frequently in phosphopeptide enrichment protocols, as phosphopeptides are generally acidic. Phosphopeptides interact poorly with the anionic stationary phase, and thus elute early compared to non-phosphorylated peptides. Hydrophilic interaction chromatography (HILIC) may be used for phosphopeptide enrichment. HILIC which uses normal phase chromatography, can enrich phosphopeptides at the end of the gradient [30]. Similarly, a variation of HILIC, ERLIC uses electrostatic repulsion to enhance separation between phosphorylated and non-phosphorylated peptides, such that phosphopeptides are retained under low pH, high organic solvent conditions [31]. Therefore, the mTMT/phos9 assay described above can be used to assess these, among other, phosphopeptide enrichment strategies.

Although the phos9 peptides were chosen as among the peptides with the highest precursor signal in a TiO<sub>2</sub>-based phosphopeptide enrichment experiment, our results showed the higher recovery with High-Select Fe-NTA than with TiO<sub>2</sub>. To reduce further selection bias, we suggest using a synthetic phosphopeptide library for future investigations, which can also include phosphorylated tyrosine. An alternative strategy could be to divide and label whole cell lysates with different mTMT reagents, thereby testing the enrichment recovery of

phosphopeptides on a global scale, and not solely as a spike-in standard as outlined herein. Even if other peptides are used, the premise of this assay remains the use of mTMT reagents to assess the recovery of selectively enriched peptides.

## CONCLUSION

Efficient binding and subsequent recovery of phosphorylated peptides from the enrichment matrix is critical for deep phosphoproteome analysis. We coupled mTMT reagents, phos9 peptides, and peak area measurements from extracted ion chromatograms to compare the phosphopeptide recovery of three enrichment methods. Our data support the notion that TiO<sub>2</sub> enrichment is hindered by low phosphopeptide recovery from the beads. From these data, it is unclear where the peptides were lost, i.e., remaining on the beads or in the unbound peptide fraction. The mTMT/phos9 assay was outlined herein can be expanded to address this question by interrogating the flow-through and wash fractions collected throughout the procedure. We foresee using mTMT for pY enrichment, as well as other posttranslational modification enrichment protocols, such as ubiquitination enrichment. The principle of these assays (i.e., measurement of mTMT labeled peptides before and after enrichment) is unaltered, only a separate set of peptides, or potentially peptide libraries, will be enrichment-specific. This assay can be used to optimize and potentially streamline experimental parameters of any enrichment strategy and in any sample background. In summary, each phosphopeptide enrichment strategy has specific advantages and disadvantages, concerning specificity, in addition to cost and duration of the procedure. Here we used mTMT and phos9 in a simple, yet versatile, internal standard-based recovery and quality control assay that offers a new metric for phosphopeptide analysis which can be applied to benchmark and enhance current phosphopeptide enrichment protocols.

## Supplementary Material

Refer to Web version on PubMed Central for supplementary material.

## Acknowledgments

### Source of Funding

This work was funded in part by an NIH/NIDDK grant K01 DK098285 (J.A.P.).

We would also like to thank members of the Gygi Lab at Harvard Medical School. This work was funded in part by an NIH/NIDDK grant K01 DK098285 (J.A.P.).

## References

1. Paulo JA, Gaun A, Gygi SP. Global Analysis of Protein Expression and Phosphorylation Levels in Nicotine-Treated Pancreatic Stellate Cells. *Journal of proteome research*. 2015; 14:4246–4256. [PubMed: 26265067]
2. Dephore N, Gould KL, Gygi SP, Kellogg DR. Mapping and analysis of phosphorylation sites: a quick guide for cell biologists. *Molecular biology of the cell*. 2013; 24:535–542. [PubMed: 23447708]
3. Wu R, Haas W, Dephore N, Huttlin EL, Zhai B, Sowa ME, Gygi SP. A large-scale method to measure absolute protein phosphorylation stoichiometries. *Nature methods*. 2011; 8:677–683. [PubMed: 21725298]

4. Wu R, Dephoure N, Haas W, Huttlin EL, Zhai B, Sowa ME, Gygi SP. Correct interpretation of comprehensive phosphorylation dynamics requires normalization by protein expression changes. *Mol Cell Proteomics*. 2011; 10:M111 009654.
5. Huttlin EL, Jedrychowski MP, Elias JE, Goswami T, Rad R, Beausoleil SA, Villen J, Haas W, Sowa ME, Gygi SP. A tissue-specific atlas of mouse protein phosphorylation and expression. *Cell*. 2010; 143:1174–1189. [PubMed: 21183079]
6. Villen J, Beausoleil SA, Gygi SP. Evaluation of the utility of neutral-loss-dependent MS3 strategies in large-scale phosphorylation analysis. *Proteomics*. 2008; 8:4444–4452. [PubMed: 18972524]
7. Repici M, Mare L, Colombo A, Ploia C, Sclip A, Bonny C, Nicod P, Salmons M, Borsello T. c-Jun N-terminal kinase binding domain-dependent phosphorylation of mitogen-activated protein kinase kinase 4 and mitogen-activated protein kinase kinase 7 and balancing cross-talk between c-Jun N-terminal kinase and extracellular signal-regulated kinase pathways in cortical neurons. *Neuroscience*. 2009; 159:94–103. [PubMed: 19135136]
8. Bahk YY, Cho IH, Kim TS. A cross-talk between oncogenic Ras and tumor suppressor PTEN through FAK Tyr861 phosphorylation in NIH/3T3 mouse embryonic fibroblasts. *Biochem Biophys Res Commun*. 2008; 377:1199–1204. [PubMed: 19000654]
9. Katsanakis KD, Pillay TS. Cross-talk between the two divergent insulin signaling pathways is revealed by the protein kinase B (Akt)-mediated phosphorylation of adapter protein APS on serine 588. *J Biol Chem*. 2005; 280:37827–37832. [PubMed: 16141217]
10. Burchfield JG, Lennard AJ, Narasimhan S, Hughes WE, Wasinger VC, Corthals GL, Okuda T, Kondoh H, Biden TJ, Schmitz-Peiffer C. Akt mediates insulin-stimulated phosphorylation of Ndr2: evidence for cross-talk with protein kinase C theta. *J Biol Chem*. 2004; 279:18623–18632. [PubMed: 14985363]
11. Paulo JA, Gygi SP. A comprehensive proteomic and phosphoproteomic analysis of yeast deletion mutants of 14-3-3 orthologs and associated effects of rapamycin. *Proteomics*. 2015; 15:474–486. [PubMed: 25315811]
12. Paulo JA, McAllister FE, Everley RA, Beausoleil SA, Banks AS, Gygi SP. Effects of MEK inhibitors GSK1120212 and PD0325901 in vivo using 10-plex quantitative proteomics and phosphoproteomics. *Proteomics*. 2015; 15:462–473. [PubMed: 25195567]
13. Ficarro SB, McClelland ML, Stukenberg PT, Burke DJ, Ross MM, Shabanowitz J, Hunt DF, White FM. Phosphoproteome analysis by mass spectrometry and its application to *Saccharomyces cerevisiae*. *Nat Biotechnol*. 2002; 20:301–305. [PubMed: 11875433]
14. Pinkse MW, Uitto PM, Hilhorst MJ, Ooms B, Heck AJ. Selective isolation at the femtomole level of phosphopeptides from proteolytic digests using 2D-NanoLC-ESI-MS/MS and titanium oxide precolumns. *Anal Chem*. 2004; 76:3935–3943. [PubMed: 15253627]
15. Bodenmiller B, Mueller LN, Mueller M, Domon B, Aebersold R. Reproducible isolation of distinct, overlapping segments of the phosphoproteome. *Nat Methods*. 2007; 4:231–237. [PubMed: 17293869]
16. Beausoleil SA, Jedrychowski M, Schwartz D, Elias JE, Villen J, Li J, Cohn MA, Cantley LC, Gygi SP. Large-scale characterization of HeLa cell nuclear phosphoproteins. *Proc Natl Acad Sci U S A*. 2004; 101:12130–12135. [PubMed: 15302935]
17. Villen J, Gygi SP. The SCX/IMAC enrichment approach for global phosphorylation analysis by mass spectrometry. *Nat Protoc*. 2008; 3:1630–1638. [PubMed: 18833199]
18. Kettenbach AN, Gerber SA. Rapid and reproducible single-stage phosphopeptide enrichment of complex peptide mixtures: application to general and phosphotyrosine-specific phosphoproteomics experiments. *Analytical chemistry*. 2011; 83:7635–7644. [PubMed: 21899308]
19. DeSouza LV, Taylor AM, Li W, Minkoff MS, Romaschin AD, Colgan TJ, Siu KW. Multiple reaction monitoring of mTRAQ-labeled peptides enables absolute quantification of endogenous levels of a potential cancer marker in cancerous and normal endometrial tissues. *Journal of proteome research*. 2008; 7:3525–3534. [PubMed: 18630974]
20. Pino LK, Searle BC, Bollinger JG, Nunn B, MacLean B, MacCoss MJ. The Skyline ecosystem: Informatics for quantitative mass spectrometry proteomics. *Mass Spectrom Rev*. 2017

21. MacLean B, Tomazela DM, Shulman N, Chambers M, Finney GL, Frewen B, Kern R, Tabb DL, Liebler DC, MacCoss MJ. Skyline: an open source document editor for creating and analyzing targeted proteomics experiments. *Bioinformatics*. 2010; 26:966–968. [PubMed: 20147306]
22. Elias JE, Gygi SP. Target-decoy search strategy for mass spectrometry-based proteomics. *Methods Mol Biol*. 2010; 604:55–71. [PubMed: 20013364]
23. Elias JE, Gygi SP. Target-decoy search strategy for increased confidence in large-scale protein identifications by mass spectrometry. *Nat Methods*. 2007; 4:207–214. [PubMed: 17327847]
24. Thingholm TE, Jensen ON, Robinson PJ, Larsen MR. SIMAC (sequential elution from IMAC), a phosphoproteomics strategy for the rapid separation of monophosphorylated from multiply phosphorylated peptides. *Mol Cell Proteomics*. 2008; 7:661–671. [PubMed: 18039691]
25. Negroni L, Claverol S, Rosenbaum J, Chevet E, Bonneu M, Schmitter JM. Comparison of IMAC and MOAC for phosphopeptide enrichment by column chromatography. *Journal of chromatography*. 2012; 891–892:109–112.
26. Dehghani A, Godderz M, Winter D. Tip-Based Fractionation of Batch-Enriched Phosphopeptides Facilitates Easy and Robust Phosphoproteome Analysis. *Journal of proteome research*. 2017
27. Possemato AP, Paulo JA, Mulhern D, Guo A, Gygi SP, Beausoleil SA. Multiplexed Phosphoproteomic Profiling Using Titanium Dioxide and Immunoaffinity Enrichments Reveals Complementary Phosphorylation Events. *Journal of proteome research*. 2017; 16:1506–1514. [PubMed: 28171727]
28. Choi, J., Snovidia, SI., Bomgardner, RD., Rogers, JC. Sequential enrichment from Metal Oxide Affinity Chromatography (SMOAC), a phosphoproteomics strategy for the separation of multiply phosphorylated from monophosphorylated peptides. *American Society for Mass Spectrometry Conference*; 2017. p. WP601
29. Olsen JV, Blagoev B, Gnad F, Macek B, Kumar C, Mortensen P, Mann M. Global, in vivo, and site-specific phosphorylation dynamics in signaling networks. *Cell*. 2006; 127:635–648. [PubMed: 17081983]
30. Boersema PJ, Mohammed S, Heck AJ. Hydrophilic interaction liquid chromatography (HILIC) in proteomics. *Anal Bioanal Chem*. 2008; 391:151–159. [PubMed: 18264818]
31. Alpert AJ. Electrostatic repulsion hydrophilic interaction chromatography for isocratic separation of charged solutes and selective isolation of phosphopeptides. *Analytical chemistry*. 2008; 80:62–76. [PubMed: 18027909]
32. Paulo JA, Urrutia R, Banks PA, Conwell DL, Steen H. Proteomic analysis of a rat pancreatic stellate cell line using liquid chromatography tandem mass spectrometry (LC-MS/MS). *J Proteomics*. 2011; 75:708–717. [PubMed: 21968429]
33. Paulo JA, Urrutia R, Banks PA, Conwell DL, Steen H. Proteomic analysis of an immortalized mouse pancreatic stellate cell line identifies differentially-expressed proteins in activated vs nonproliferating cell states. *Journal of proteome research*. 2011; 10:4835–4844. [PubMed: 21838295]



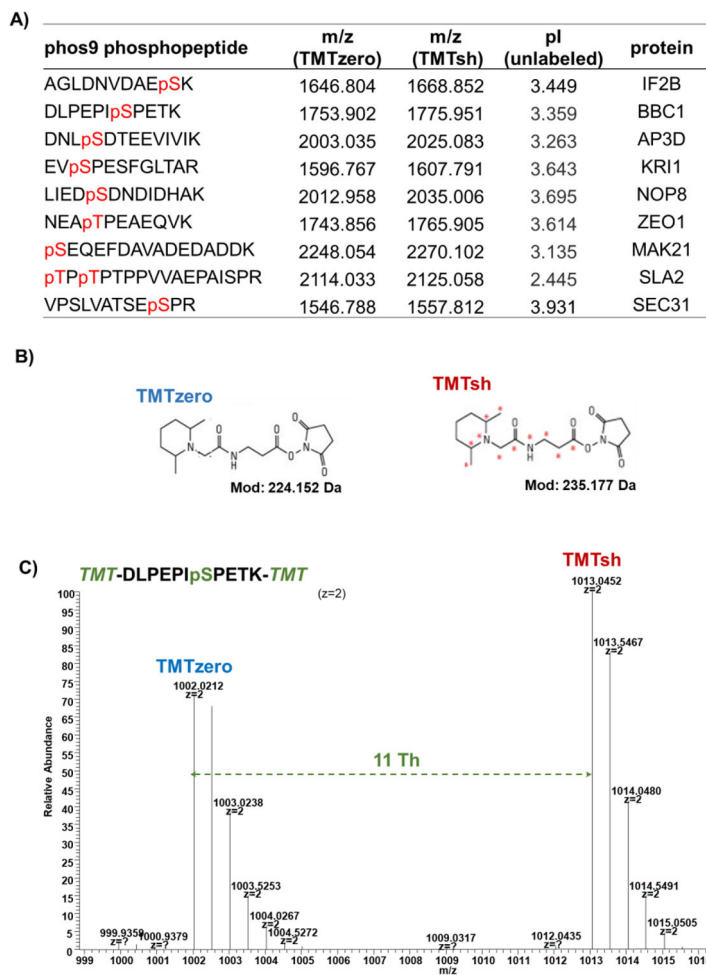


**Figure 1. TMT reagents and peptides used in this experiment**

**A)** The table lists the phos9 phosphopeptide sequences, m/z for TMTzero- and TMTsh-labeled phosphopeptides, isoelectric point for unlabeled phosphopeptide, and associated protein. **B)** Chemical structures of TMTzero and TMTsh. **C)** Spectrum highlighting the mass difference between a doubly charged, lysine-terminating peptide (DLPEI

I

pSPETK) labeled with TMTzero and TMTsh.

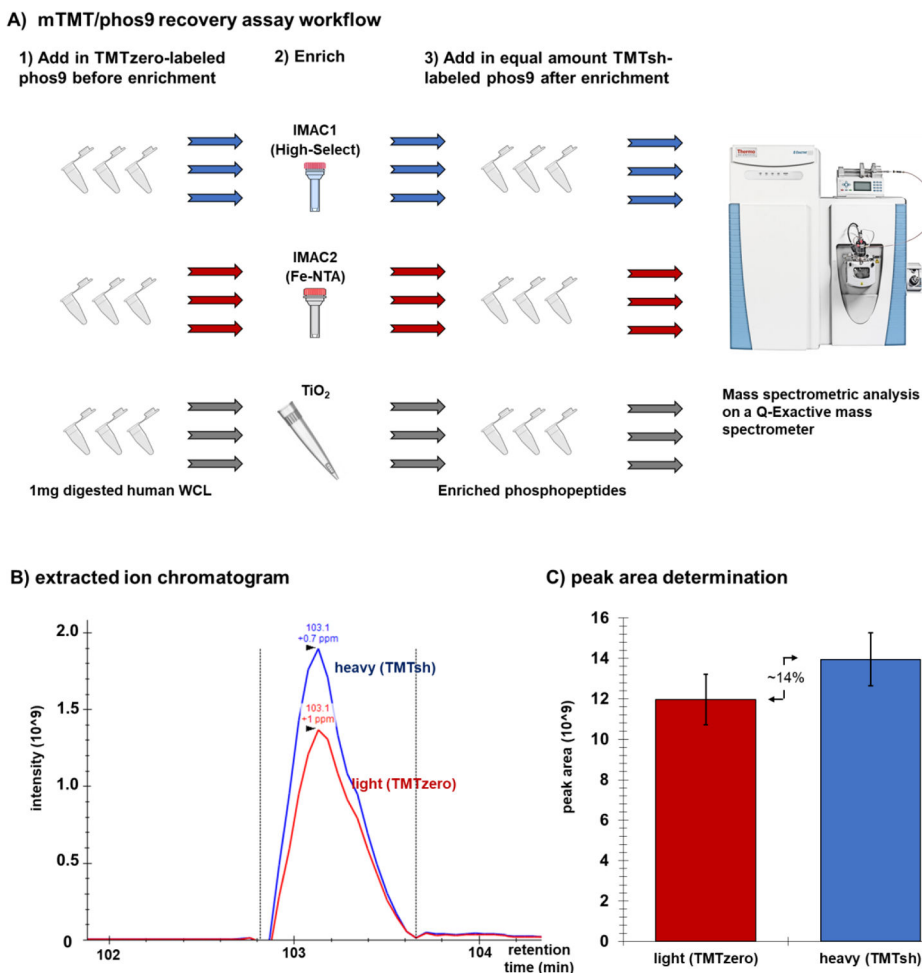


**Figure 2. Experimental overview of phosphopeptide enrichment strategy**

**A)** TMTzero-labeled phos9 was added to 1mg aliquots of trypsinized human whole cell lysate (WCL). Phosphopeptides were enriched using one of three methods (High-Select, Fe-NTA, TiO<sub>2</sub>) with three technical replicates. TMTsh-labeled phos9 was spiked into the enriched sample. The sample was desalted and analyzed on a QExactive mass spectrometer. **B)** Example of an extracted ion chromatogram, as displayed in Skyline. **C)** Peak area comparison as determined in Skyline.

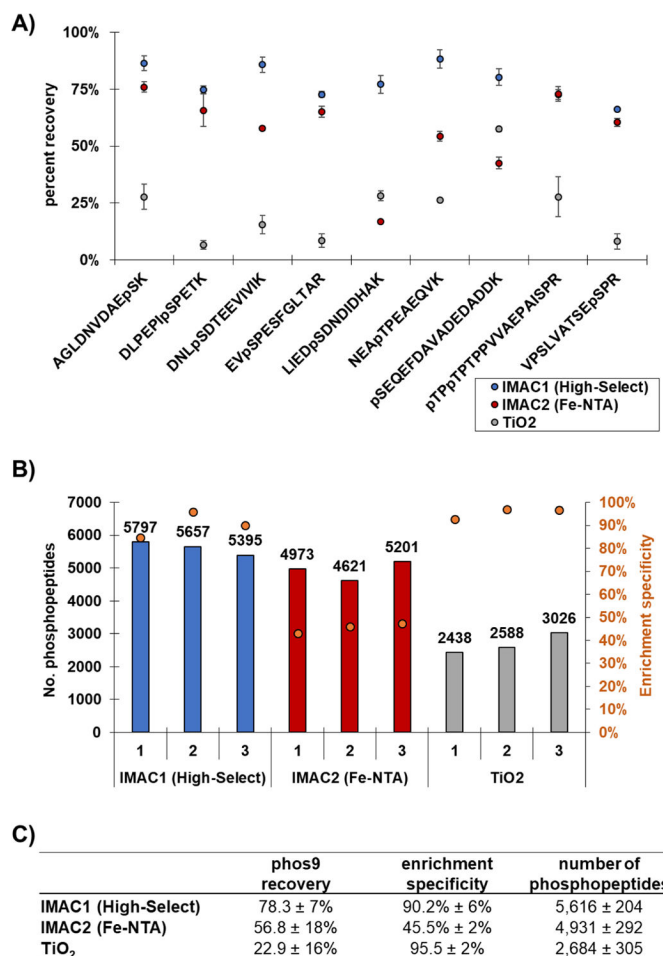


**Figure 3. Evaluation of phosphorylated peptides identified by each enrichment method**

**A)** The dot plot illustrates the efficiency of recovery (peak area ratio of TMTzero to TMTsh) for phos9 phosphopeptides. Error bars represent standard error of the mean (s.e.m.) for three independent replicate samples. **B)** The bar plot illustrates the total number of phosphorylated peptides identified by each method. The overlaid orange circles represent the enrichment specificity (percentage of peptides that are phosphorylated) for each method. **C)** The table summarizes the findings for the phos9 peptide cocktail (mean ± SD).